Still "Plenty of Room at the Bottom" for Aberration-Corrected TEM

Joerg R. Jinschek,[1] * Emrah Yucelen,[1 2] Bert Freitag,[1] Hector A. Calderon,[3] and Andy Steinbach[1]

[1] FEI Company, Europe NanoPort, Achtseweg Noord 5, 5651 GG Eindhoven, The Netherlands
[2] National Centre for HREM, Delft University of Technology, Lorentzweg 1, 2628 CJ, Delft, The Netherlands
[3] ESFM-IPN, UPALM ed. 9, Zacatenco DF 07738 Mexico City, Mexico

* joerg.jinschek@fei.com

Introduction

In his now-famous 1959 speech on nanotechnology [1], Richard Feynman proposed that it should be possible to see the individual atoms in a material, if only the electron microscope could be made 100 times better. With the development of aberration correctors on transmission electron microscopes (TEMs) over the last decade, this dream of microscopists to directly image structures atom-by-atom has come close to an everyday reality. Figure 1 shows such a high-resolution transmission electron microscope (HR-TEM) image of a single-wall carbon nanotube obtained with an aberration-corrected TEM. Now that atomic-resolution images have become possible with aberration-corrector technology in both TEM and STEM, we can ask ourselves if we truly have achieved the goal of seeing individual atoms. Most aberration-corrected images exhibiting atomic resolution are not distinguishing individual atoms, but columns of a small number of atoms, so despite this remarkable achievement, there is *still* "plenty of room at the bottom" in order to move toward seeing, counting, and quantifying individual atoms.

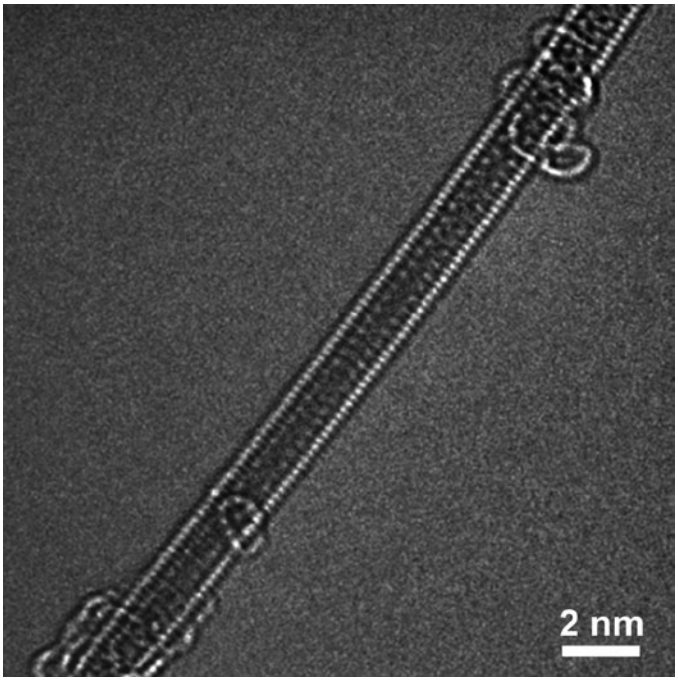

Figure 1: Aberration-corrected HR-TEM image of a single-walled carbon nanotube, obtained at 80 kV accelerating voltage. Image: Bert Freitag, FEI; sample: Professor Kiselev, Moscow, Russia.

In fact, there never has been a more exciting time for electron microscopists.

In this article we discuss one of the exciting new technical frontiers that is pushing toward quantitative, atomic imaging in all three dimensions. We describe one technique for performing quantitative atomic 3-D imaging using focal series reconstruction (FSR) [2] with aberration-corrected HR-TEM images [3]. We show that when the remaining small residual aberrations are removed, we can easily resolve individual atoms (as opposed to atom columns) with atomic resolution in three dimensions and unprecedented signal-to-noise ratio, even for beam-sensitive structures requiring lower accelerating voltages. This technique is demonstrated via an HR-TEM study using a specimen of single- and double-layer graphene at 80 kV accelerating voltage [4].

Ideal HR-TEM Imaging Theory

Figure 2 depicts the theoretical, electron-wave basis for quantitative HR-TEM imaging (after [5]). In figure 2a we see that when the electron wave passes from vacuum to the denser material of a single atom, the wavelength shortens. In figure 2b, the horizontal lines represent the plane-wave surfaces of constant electron phase, and we see that the effect of an atom on the wave is to retard or delay the electron phase (just as in light optics; when entering a material the speed of the light wave slows down, while its frequency remains constant, thus yielding an effectively shorter wavelength.) So the electron wave phase front "bends" around the electric potential of the screened atomic core as it passes an atom. Figure 2c depicts the evolving electron phase in a thin sample with several atoms. As the wave exits the sample, all of the sample information collected by the electron wave is contained in the so-called exit-wave phase (EW phase), which is simply the electron phase as a function of position just below the sample. In a very thin sample, only the electron wave's phase is affected by passage through the sample, whereas the amplitude remains unchanged. This fact is reflected in the so-called phase object approximation [6]. The EW phase is then given by the formula:

$$\varphi_{Exit\ Wave}(x,y) = \int_0^{Exit} V(x,y,z)\,dz \qquad (1)$$

where V is the electric potential of the atomic structure within the sample. So the exit phase is proportional to the electric potential integrated along z (that is, from the top to the bottom of the sample). Using 3-D structural models, the theoretical exit wave can thus be simulated and used for comparison with the real structure. The experimental EW phase function is extremely valuable; in fact, if we can obtain it with atomic

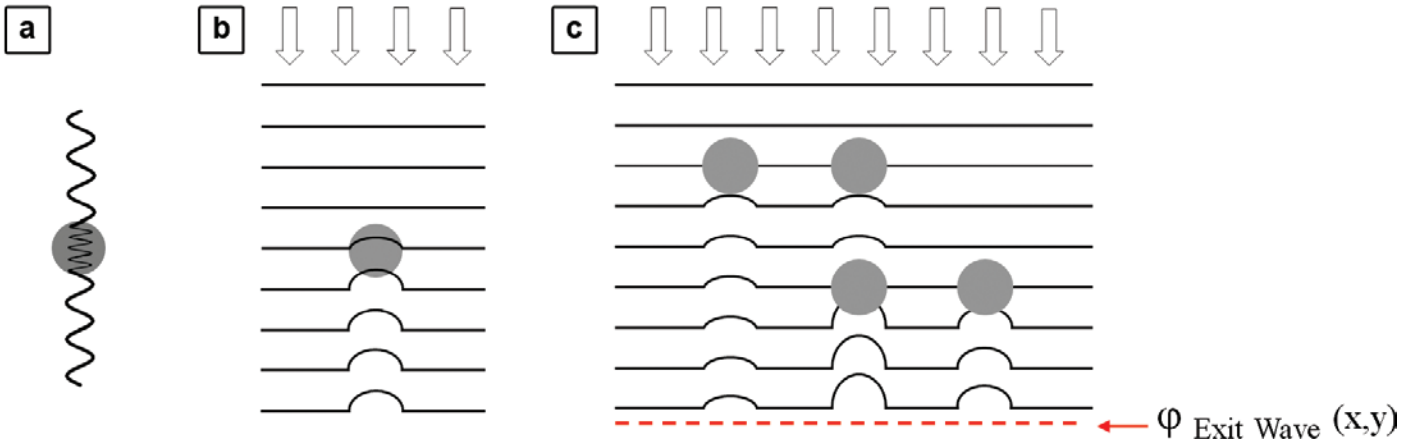

Figure 2: Theoretical electron-wave basis for HR-TEM imaging, showing (a) change in electron wavelength due to material density, (b) electron phase-front delay or "bending" due to passage through an atom, and (c) effect on electron EW phase-front in a sample with several atoms (after [5]).

resolution and high signal-to-noise ratio, we can actually count individual atoms and ultimately infer their vertical position in the 3-D structure.

Complications Due to the Non-Ideal TEM

In an *ideal* TEM, this desired sample EW phase would be perfectly magnified by the microscope without any aberration, by a large scaling factor M (such as 500,000×) and then somehow recorded after this magnification process. In a *real* microscope (see Figure 3), at least two complications prevent this from happening directly: (a) the magnified image, even in an HR-TEM microscope with hardware C_s-correction, still has residual aberrations, and (b) typical image recording methods such as CCD camera are not capable of detecting electron phase, but only electron intensity (essentially the amplitude squared). As noted above, for a very thin sample, the amplitude does not change during the electron-sample interaction. A true aberration-free microscope would have zero image contrast in HR-TEM because it measures only the amplitude, which does not change! Luckily, in this case, the microscope aberrations actually help us in our task to image the sample. The effect of the microscope optical aberrations is to "couple" or mix the exit-wave amplitude and phase [7]. This scrambling ensures that there is some contrast change in the electron amplitude at the image plane of the CCD camera.

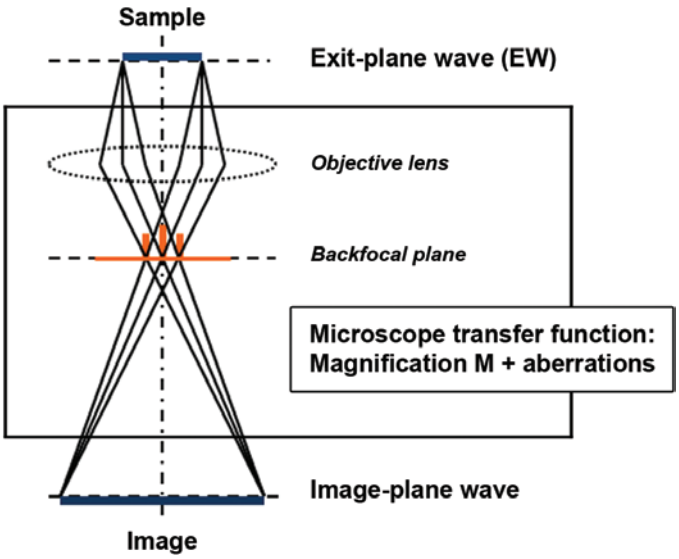

Figure 3: HR-TEM schematic. An ideal TEM would magnify the sample exit-wave information by a large magnification factor M, but the electron optics of a real microscope will also introduce aberrations in the image recorded at the image plane. This optical transfer function, including residual aberrations, can be deconvolved by using FSR as described in the text (after H. Lichte, TU Dresden).

Deconvolving the Microscope Transfer Function

Imaging in the HR-TEM is an electron wave-coherent process, so if we know the microscope's exact optical parameters, theoretically we should be able to mathematically deconvolve the scrambling of phase and amplitude to get back to the desired pure EW phase function. Focal series reconstruction (FSR) is a technique [2, 8] used to perform this deconvolution of amplitude and phase. It requires a series of HR-TEM CCD images; typically up to twenty individual images, each taken at a different numerical value of defocus (around the real focus value). Although the signal-to-noise ratio can be improved by averaging [9], this operation is more than just averaging twenty images to improve signal-to-noise ratio: by changing the experimental focus and feeding the known microscope optical parameters into a numerical FSR calculation, the FSR program can deconvolve or "subtract" the microscope's optical transfer function. The result is that the software [8] can output two processed experimental images, the pure EW phase and the exit-wave amplitude, with the scrambling effect fully unraveled. In the limit of a very thin sample and perfect deconvolution, the EW amplitude goes virtually to zero, leaving only the desired EW phase information.

Imaging of Graphene: Experimental Setup and Details

For this HR-TEM study, graphene sheets were carefully prepared [4], and the experiments were performed using an FEI Titan G2 60-300 microscope operated at 80 kV, equipped with a high-brightness, low-energy-spread X-FEG/monochromated field-emission electron source, as well as a CEOS aberration corrector to correct the spherical aberration of the objective lens. The CEOS aberration corrector was tuned to a spherical aberration C_s value of about –15 µm (to optimize the details in the image intensity) [10].

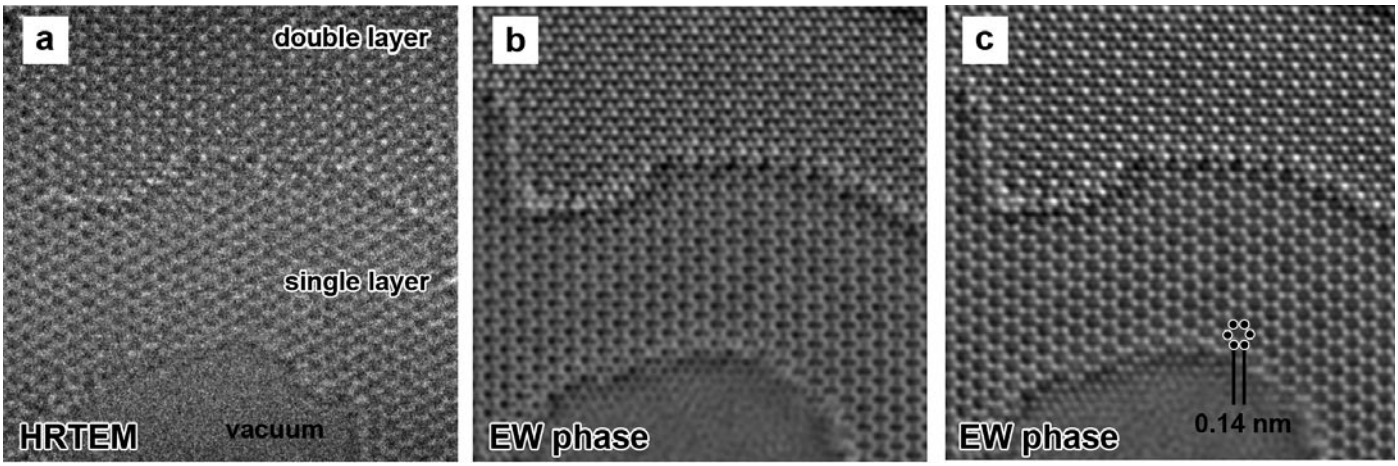

Figure 4: Figures (a–c) show the subsequent improvement in imaging of the same graphene sample by the process described in the text: (a) a raw aberration-corrected TEM CCD image of the sample at 0.1 s exposure time, (b) an EW phase image obtained through FSR of 19 such raw images at constant focal step, and (c) the FSR EW phase image from (b) with residual aberrations numerically removed [4].

For beam-sensitive soft materials like graphene, the low threshold for "knock-on" damage (where atoms are ejected by the energetic electron beam, estimated to be about 113 keV for graphene) requires a low accelerating voltage, such as 80 kV. This has advantages because electron scattering becomes stronger at lower accelerating voltages, but it also has disadvantages because resolution decreases and residual aberrations increase at lower voltage. At such low voltages, the electron beam energy spread becomes the spatial-resolution limiting parameter in a microscope corrected for spherical aberration but not chromatic aberration [11]. This experiment was conducted with an energy spread slightly below 0.2 eV leading to an achievable spatial resolution of at least 0.11 nm (1.1 Å) or better, which is important for this study so that the C–C bond length in graphene of 0.142 nm (1.42 Å) can be well-resolved.

The Graphene Study: Experimentally Reconstructed Focal Series Results

A FSR of the graphene sample EW phase and exit-wave amplitude has been performed using FEI's TrueImage software [8]. The images were recorded with a 2k × 2k pixel CCD array using a short acquisition time of 0.1 second per image, chosen to fulfill dose constraints and also to minimize the likelihood of atomic-level damage or motion of the sample during the full series of 19 images. A focal step of –1.9 nm/image was used, and, importantly, the sampling on the CCD camera was set to 0.0094 nm/pixel.

Figure 4a shows a single HR-TEM CCD image of the sample, which includes an area of both double- and single-layer graphene, as well as a region of "vacuum" (that is, a hole in the single-layer structure). Although this image is noisy, nonetheless a hint of the hexagonal lattice structure begins to emerge in the single-layer region. However, the appearance of this type of CCD image depends on the exact value of defocus. Thus, for unambiguous comparison with theory, one should ideally work with the EW phase, which is shown in Figure 4b, obtained via FSR on the nineteen CCD images as described above. Although Figure 4b appears to be less noisy than Figure 4a, there is still a residual blur in the single-layer region that does not permit an unambiguous interpretation of the hexagonal atomic structure of single-layer graphene. This blur is due to residual aberrations and not the presence of noise. Proof of this statement is seen in Figure 4c, in which the residual optical aberrations have been numerically removed from the EW phase image using the TrueImage software. The final result shown in Figure 4c is the experimental EW phase image of the sample corrected for residual aberrations. In this final image, the well-known hexagonal arrangement of single carbon atoms in the single-layer graphene is very clearly resolved. In the next section, we explain the theoretical model that was used for comparison with the experimental results and the method that was used to remove the residual aberrations.

The New Frontier: Eliminating Residual Aberrations After Aberration Correction

Figure 4c shows a numerically reconstructed experimental EW phase image, which appears to show an area of double-layer graphene at the top and a single-layer in the area in the lower half of the image. In order to compare these data with theoretical expectations, a numerical simulation was performed using the multi-slice algorithm in the MacTempas software by Total Resolution LLC [12]. Figure 5a shows a sketch of the input structural model to the simulation program to

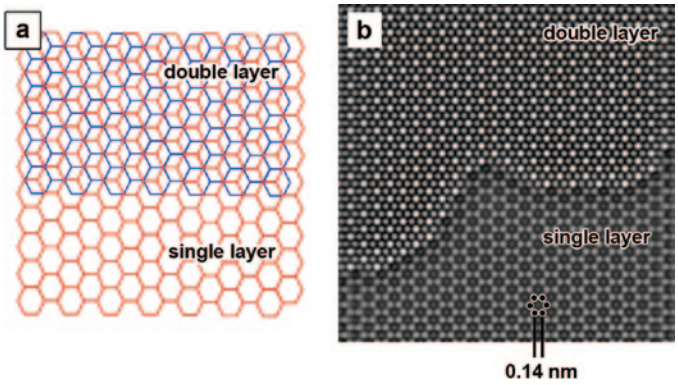

Figure 5: (a) Schematic of the model structure for the graphene sample used as input to the simulation. (b) The EW phase image of the simulated model structure, containing both areas of double- and single-layer graphene, similar to the actual sample in the experimental study [4].

model the double-layer graphene: two hexagonal graphene sheets are overlaid in a so-called Bernal-stacked alignment. Figure 5b shows the EW phase for the simulation result, which is modeled with zero noise and zero aberrations. The simulated single-layer graphene looks perfectly like its known hexagonal model structure, with bright spots representing single carbon atoms. The experimentally reconstructed EW phase image in figure 4c strongly resembles the simulation; thus, the FSR has allowed us to clearly identify areas of single and double sheets and to confirm the type of stacking alignment. The apparent visible structure in Figure 4c at the boundary between vacuum and the single layer is an artifact due to atomic-level motion or evolution of individual edge atoms during the focal series. Because the edge is not a topic of study, this does not affect the results in this review. In figure 6, we provide a more detailed comparison between the simulated model and the experimental results.

The application of FSR discussed above provides an unscrambled, experimental EW phase function that can be directly compared with theoretical structural studies calculated from Equation (1), such as those calculated in Figure 5b. However, the initially reconstructed EW phase obtained by FSR in Figure 4b contained blur attributable to residual aberrations. In this study, we have taken an important further step by numerically deconvolving the small residual aberrations that remained after aberration correction. Having obtained by FSR the EW phase function experimentally, this further deconvolution was an "easy" subsequent task (mathematically complex, yet straightforward), but we needed to know precisely the *actual residual experimental aberrations*, either by (a) direct measurement or by (b) some kind of inference. There are direct measurement schemes for obtaining residual aberrations that we discuss below, but first we describe how the residual aberrations were inferred in the present experiment with graphene by using the known structure of the single-layer graphene essentially as a calibration standard.

The experimental residual aberrations of the microscope for this focal series were found by adjusting the aberration coefficients up to third order in the TrueImage software [8] and then using the software to numerically "subtract" these aberrations from the experimental EW phase. The coefficients were adjusted using a best-fit iterative approach until the new corrected experimental result closely matched the calculated image in Figure 5b for the theoretical EW phase of graphene in the single-layer region.

Figure 4c shows the resulting experimental EW phase after this numerical subtraction of residual aberrations. The single-layer graphene area has converged (because of the aberration coefficient best fit) to an almost noise-free representation of the graphene hexagonal lattice. The match between the EW phase of the numerically simulated model structure (calculated by a multi-slice implementation [13] of Equation (1) using the detailed model input structure shown as a caricature in Figure 5a) and the experimental EW phase results of Figure 4c is quite remarkable. This confirms that the actual sample structure in the double-layer area is in fact the Bernal-stacking alignment that was programmed into the model simulation as input on the structure.

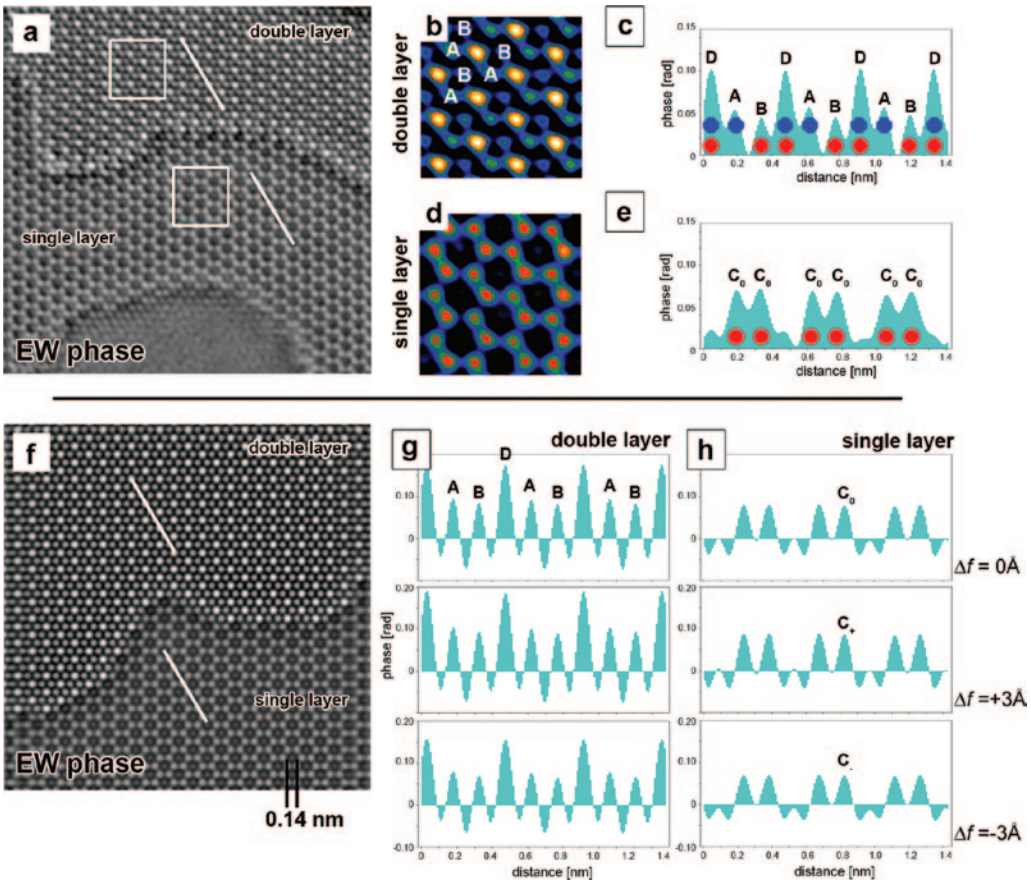

Figure 6: (a) Experimental EW phase images of graphene sheets—the same as Figure 4c (right side). (b and d) Higher magnification in RGB color scale: (b) from the double-layer area; (d) from the single-layer area, indicated by ''h'' in (a). (c and e) Line scans of experimental phase image: (c) from the double-layer area; (e) from the single-layer area. (f) Simulated EW phase image of graphene sheet(s)—the same as Figure 5b. (g and h) Line scans (as indicated in (f) in ''double layer'' and ''single layer'' region) on EW phase images propagated by a defocus of +3 Å and –3 Å [4].

The Final Result: Extracting Quantitative 3-D Information at the Atomic Scale

Figure 6a shows the same EW phase experimental result as in Figure 4c, but with additional quantitative analysis [4]. The two square sample areas marked in Figure 6a are shown in the color maps in figures 6b and 6d. The brightest orange spots in Figure 6b represent the two-carbon-atom atomic columns in the double-layer graphene structure and therefore represent the

largest phase shift in the EW phase map. The atomic locations marked "A" and "B" in Figure 6b are clearly distinguished by different peak values in the EW phase map, and these peaks represent the location of single carbon atoms in either the top or bottom graphene. The average value of the EW phase of the carbon atoms in the "A" indexed locations is 9.5 percent larger than the phase shift value at the "B" indexed locations. This is clearly above the 2.3 percent noise level estimated from shot noise considerations calculated from the experimental dose rate. Further, the line scan in Figure 6e shows that a typical difference in phase between atomic peaks in the single-layer area, due to uncorrected residual aberrations, is significantly smaller (0.002 radians = noise level) than the phase difference between carbon atoms belonging to the two different layers (top versus bottom) in the double-layer region (average signal = 0.010 radians). The fundamental measurement units of the EW phase are given as an angle measured in radians. This can be understood as one full cycle of an electron spatial wavelength representing 360 degrees or 2π radians because the relativistic electron wavelength at the chosen accelerating voltage is the "measuring stick" we are using on the atomic structure. So a noise level of 0.002 radians means that we are measuring with an uncertainty of only ~0.1 degrees in the wavelength's angular cycle! As a further comparison between theory and experiment, line scan analyses (indicated in Figure 6f) on the simulated model structure predict that there is a 0.014-radian phase difference between the single-C-atom "columns" depending on whether they are in the top layer or the bottom sheet (marked "A" or "B" respectively in the line scan data in Figure 6g). The difference in height in the beam direction of these two atomic positions is 3.5 Angstroms. Finally, the simulation was run with a defocus change of both +3 Å and –3 Å. In the single-layer area, the line scan in Figure 6h shows that the predicted simulated phase change for this focus change (equivalent to moving a carbon atom by the same amount) is +0.010 rad (for +3 Å defocus) and –0.014 rad (for –3 Å defocus). This verifies that the measurable phase difference between "A" and "B" in the experimental data is caused by the difference in upper/lower sheet position in the double-layer area.

Conclusion and Future Prospects

This graphene study [4] has shown two steps of results: First, by applying FSR to HR-TEM images obtained with a aberration-corrected TEM, and taking advantage of the improved low energy-spread of a monochromated source, we are able to obtain the fundamental experimental quantity known as the EW phase for a sample containing both single- and double-layer graphene structure. As a second step, the small residual microscope aberrations were inferred and numerically removed from this EW phase, resulting in unprecedented imaging of the same structure. The final result demonstrates an ability to numerically verify the positions of the atoms in all three dimensions, even in the vertical direction differentiating 3A height differences with high signal fidelity.

In this study, it was possible to obtain the residual aberrations using single-layer graphene as a known "calibration structure," but for many samples this would not be possible. Therefore, it would be desirable to have a procedure to *measure* the residual aberrations of the C_s aberration corrector at a given time. The aberrations could then be directly subtracted (or deconvolved) from the EW phase function, allowing the level of imaging quality in this study to be repeated on a wider range of samples and structures, including wholly unknown structures without the equivalent of a graphene "single-layer calibration." Methods for measuring with high accuracy the corrector's residual aberrations via software are under development. Soon it should be possible to use these methods via automated algorithms to measure the actual residual aberrations of the corrected microscope [13]. This will allow residual aberrations to be directly measured and numerically deconvolved for a greater range of samples and experimental conditions. For example, recent studies of graphene with nitrogen doping provide evidence that HR-TEM studies can record changes in electron density due to chemical bonding [14], and it may be possible that the techniques described in this review could enable experimental studies that would further shed light on this exciting new topic, just to give one example of potential future directions of investigation.

Acknowledgments

The authors would like to thank Edgar Voelkl for helpful comments on this article.

References

[1] "There's Plenty of Room at the Bottom," a speech given by physicist R.P. Feynman at a meeting of the American Physical Society at California Institute of Technology, December 29, 1959.

[2] W Coene, A Thust, M Op de Beeck, and D Van Dyck, *Ultramicroscopy* 64 (1996) 109–35; and A Thust, WMJ Coene, M Op de Beek, and D van Dyck, *Ultramicroscopy* 64 (1996) 211–30.

[3] M Haider, S Uhlemann, E Schwan, H Rose, B Kabius, and K Urban, *Nature* 392 (1998) 768–69.

[4] JR Jinschek, E Yucelen, HA Calderon, and B Freitag, *Carbon* 49 (2011) 556–62.

[5] A Thust, *Microsc Microanal* 11 (Suppl 2) (2005) 602–03.

[6] DB Williams and CB Carter, *Transmission Electron Microscopy—A Textbook for Materials Science*, Plenum Press, New York, 1996, p. 461.

[7] L Reimer and H Kohl, *Transmission Electron Microscopy: Physics of Image Formation*, 5th ed., Springer Science, New York, 2005.

[8] P Schlossmacher, Ch Kuebel, B Freitag, D Hubert, and R Perquin, *Microsc Microanal* 13 (Suppl 2) (2007) 1170–71.

[9] E Voelkl, B Jiang, ZR Dai, and JP Bradley, *Microscopy Today* 16(6) (2008) 36–38.

[10] C-L Jia, M Lentzen, K Urban, *Microsc Microanal* 10 (2004) 174–84.

[11] J Barthel and A Thust, *Phys Rev Lett* 101(20) (2008) 200801.

[12] R Kilaas, "HREM image simulation" in *Proceeding of 49th EMSA Meeting*, ed. G W Bailey, San Francisco Press, San Francisco, 1991, p. 528–29.

[13] J Barthel and A Thust, *Ultramicroscopy* 111 (2010) 27–46.

[14] JC Meyer et al., *Nature Mater* 10 (2011) 209–15.

MT

SEEING IS BELIEVING™

Quantitative *In-Situ* Tensile Testing Inside Your SEM or TEM Using Hysitron's Push-To-Pull (PTP) Device*

*Patent Pending

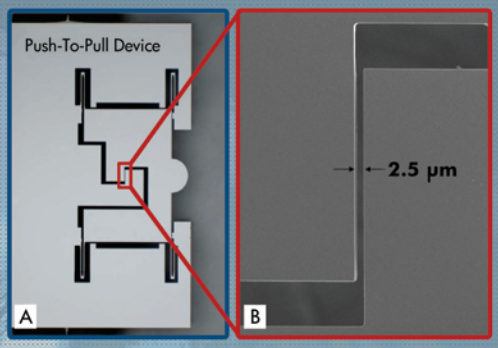

Optical Image of PTP Device

SEM Image of PTP Device Gap

- Ideal for nanowires and nanoribbons
- Quantitative load-displacement data simultaneous with real-time images of material deformation
- Convert to stress-strain curves
- Available for Hysitron's PI Series PicoIndenters
- A high-precision MEMS-fabricated device

In-Situ Tensile Test of ZnO Nanowire

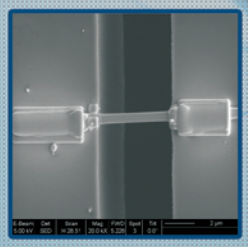

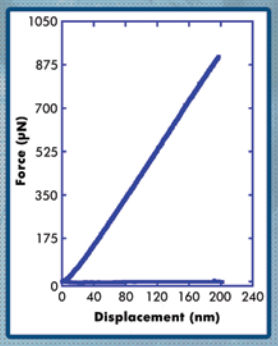

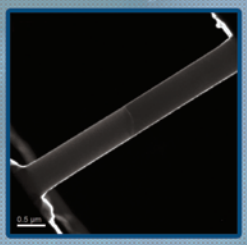

PI Series PicoIndenter™
In-situ nanomechanical testing inside your TEM or SEM
(indentation, compression, bending, tensile, etc.)

PI 95 TEM PicoIndenter™

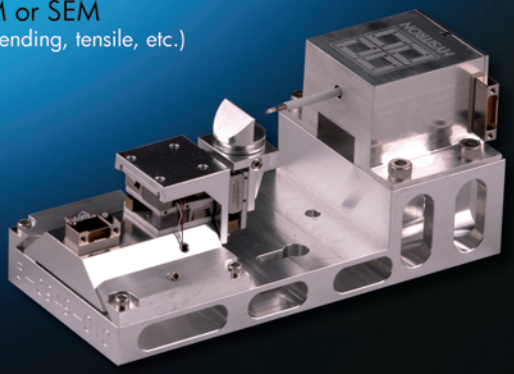

PI 85 SEM PicoIndenter™

HYSITRON™

see more @ **hysitron.com**

https://doi.org/10.1017/S155192951100023X Published online by Cambridge University Press